Journal Pre-proof

The application years of biochar affect CH_4 emission by negatively methanogens and increased rice yield

Kai Zhang, Zhongcheng Zhang, Yanghui Sui, Jialing Wang, Xiaobo Pei, Yanze Zhao, Jiping Gao, Wenzhong Zhang

PII: S2352-1864(25)00085-9
DOI: https://doi.org/10.1016/j.eti.2025.104099
Reference: ETI104099

To appear in: *Environmental Technology & Innovation*

Received date: 18 December 2024
Revised date: 8 February 2025
Accepted date: 19 February 2025

Please cite this article as: Kai Zhang, Zhongcheng Zhang, Yanghui Sui, Jialing Wang, Xiaobo Pei, Yanze Zhao, Jiping Gao and Wenzhong Zhang, The application years of biochar affect CH_4 emission by negatively methanogens and increased rice yield, *Environmental Technology & Innovation,* (2025) doi:https://doi.org/10.1016/j.eti.2025.104099

This is a PDF file of an article that has undergone enhancements after acceptance, such as the addition of a cover page and metadata, and formatting for readability, but it is not yet the definitive version of record. This version will undergo additional copyediting, typesetting and review before it is published in its final form, but we are providing this version to give early visibility of the article. Please note that, during the production process, errors may be discovered which could affect the content, and all legal disclaimers that apply to the journal pertain.

© 2025 Published by Elsevier.

The application years of biochar affect CH_4 emission by negatively methanogens and increased rice yield

Kai Zhang [a,1], Zhongcheng Zhang [a,1], Yanghui Sui [b,1], Jialing Wang [a], Xiaobo Pei [a], Yanze Zhao [a], Jiping Gao [a, *], Wenzhong Zhang [a]

[a] Rice Research Institute, Shenyang Agricultural University/National and Local Joint Engineering Laboratory of Japonica Rice Breeding and Cultivation Technology in North China, Shenyang 110866, China

[b] Corn Research Institute, Liaoning Academy of Agricultural Sciences, Shenyang110161, China;

[*] Corresponding author.

E-mail address: jipinggao@syau.edu.cn (J. Gao).

[1] These authors contributed equally to this work.

Journal Pre-proof

Abstract

Biochar influences CH_4 emissions, methane-associated microbial communities, and rice yields. However, the effects of biochar application over different durations remain unclear. This study investigated the impact of biochar application on CH_4 emissions, methane-associated microbial communities, and rice yield across different years. Five treatments were assessed based on the year of biochar application (NB: applied in April 2023; FB: applied in April 2016) along with three biochar application rates (CK: 0 $t{\cdot}ha^{-1}$; NB15, FB15: 15 $t{\cdot}ha^{-1}$; NB45, FB45: 45 $t{\cdot}ha^{-1}$). Biochar application improved the physical and chemical properties of the soil, with NB45 exhibiting the most pronounced effect. Compared with CK, CH_4 emissions increased under NB conditions but decreased under FB conditions. Additionally, emissions were higher at lower biochar application rates than at higher rates across all years. These trends were associated with shifts in the abundance of methanogenic and methane-oxidising bacteria in the soil. Biochar reduced the *pmoA*/*mcrA* ratio in paddy soil, with FB45 showing the greatest reduction. The composition of methanogenic and methane-oxidising bacterial species differed significantly between NB and FB soils, with *Chloroflexota* exhibiting the highest relative abundance in both bacterial groups. Biochar application enhanced CH_4 metabolism in methanogenic and methane-oxidising bacteria, with the strongest effect observed under the NB treatment. Moreover, biochar application significantly improved rice yield, increasing by 9.27%, 12.58%, 13.50%, and 14.68% under the NB15, NB45, FB15, and FB45 treatments, respectively. Overall, biochar effectively reduced CH_4 emissions, modulated the structure and function of methane-associated microbial communities, and enhanced rice yield.

Keywords: Duration of biochar application; CH_4 emissions; Methanogenic bacteria; Methane oxidising bacteria; Rice yield

1. Introduction

Global warming, driven by greenhouse gas (GHG) emissions, is a major factor contributing to the decline in food production due to extreme weather events (Shahid et al., 2023). The cumulative emissions of carbon dioxide (CO_2), methane (CH_4), and nitrous oxide (N_2O), the primary GHGs, increased by approximately 5.6%, 4.2%, and 2.7%, respectively, between 2011 and 2020 (Shrestha et al., 2023). GHG emissions from paddy fields account for 40.9% of total agricultural GHG emissions (Wu et al., 2022). CH_4 is the second most significant GHG, contributing to approximately one-third of current anthropogenic warming. Although its atmospheric concentration is < 0.5% that of CO_2, CH_4 is a far more potent GHG, with a global warming potential 27 times greater than CO_2 over a 100-year period and 80 times greater over 20 years (Xin et al., 2023). CH_4 from rice cultivation constitutes more than 20% of agricultural CH_4 emissions (Perry et al., 2024). As a critical component of GHGs, CH_4 has profound effects on global climate and environmental changes. Consequently, reducing CH_4 emissions from rice cultivation has become a key research priority.

Mitigating CH_4 emissions from agricultural land is essential for addressing climate change and achieving carbon neutrality targets (Tian et al., 2024). CH_4 emissions are directly regulated by methanogens and methanotrophs (Chen et al., 2023). All known methanogens belong to the phylum Euryarchaeota (Archaea), which is divided into seven orders: *Methanosarcinales, Methanocellales, Methanobacteriales, Methanococcales, Methanomicrobiales, Methanomassiliicoccales*, and *Methanopyrales* (Luo et al., 2022). At the genus level, *Methanothrix, Methanobacterium, Methanosarcina,* and *Methanocella* are the predominant methanogens in paddy fields (Jiang et al., 2022). Methanogens play a crucial role in CH_4 production, as organic matter in paddy soil is anaerobically degraded by various bacteria into CH_4 precursors, which are then converted to CH_4, by methanogenic bacteria (Gao et al., 2022). Conversely, a class of microorganisms known as methane-oxidising bacteria (methanotrophs) can oxidise CH_4 to carbon monoxide (CO), significantly reducing CH_4 emissions from paddy fields (Schorn et al., 2024). Methanotrophs utilise CH_4 as their sole carbon and energy source, converting it into methanol (Patel et al., 2020). The dominant methanotrophs at the genus level are *Methylocystis, Methylococcus, Methylocaldum,* and *Methylosarcina* (Yu et al., 2023). These microorganisms play a vital role in CH_4 mitigation in soil ecosystems (Heděnec et al., 2024).

Biochar is a carbon-rich, stabilised by-product produced through the pyrolysis of biomass (e.g., agricultural and forestry residues) under anaerobic conditions. It is characterised by a rich, porous

Journal Pre-proof

Journal Pre-proof

structure and stable physicochemical properties (Li et al., 2024). Biochar has the ability to improve the physical and chemical properties of soil (Khan et al., 2024). The application of biochar as an organic amendment has been recognised as a potential agronomic measure with the dual ecological benefits of increased crop yields and reduced greenhouse gas emissions (Zhao et al., 2024; Dai et al., 2024). Recent research has demonstrated that the application of corn stover biochar reduced CH_4 emissions by 39.74% in large-scale field trials (Zhao et al., 2023). This reduction is attributed to biochar's ability to modulate microbial communities, enhance the abundance of methane-oxidising bacteria, and regulate the ratio of methanogenic to methane-oxidising bacteria (Qi et al., 2021; Qin et al., 2016). While much research has focused on the short-term effects of biochar application on CH_4 emissions and microbial community structure, it is equally important to assess its long-term impacts. The physicochemical properties of biochar evolve over time due to various abiotic (e.g., temperature fluctuations, rainfall, and light exposure) and biotic (plants, soil fauna, and microorganisms) factors (Long et al., 2024; Quilliam et al., 2013). Over time, the microbial community in the soil becomes more enriched, potentially leading to enhanced CH_4 mitigation (Zhou et al., 2023; Bo et al., 2023). Previous studies have reported an 11% reduction in CH_4 emissions from rice paddies several years after biochar application (Feng et al., 2022). However, contradictory findings have also been reported. Some studies suggest that the liming effect of biochar, which initially promotes methane oxidation by creating a favourable environment for methanotrophs, diminishes over time, thereby weakening its ability to enhance methane oxidation (Nan et al., 2021). Additionally, other studies have found no significant many years after the addition of biochar on CH_4 emissions, in contrast to its initial impact (Spokas, 2013). To better understand whether biochar has the potential for long-term CH_4 emission reduction and microbial community modulation, further investigation is required. It is necessary to evaluate both the immediate effects of biochar application and many years after the addition of biochar on CH_4 emissions and methane-associated microbial communities.

This study is based on the hypothesis that different biochar application durations and amounts regulate methanogen and methanotroph gene abundance in paddy fields, thereby reducing CH_4 emissions, improving soil physicochemical properties, and increasing rice yields. To test this hypothesis, Illumina HiSeq sequencing technology was employed to analyse the composition and function of methanogens and methanotrophs in paddy soil. The significance of biochar application duration in CH_4 mitigation was explored from a soil micro-ecosystem perspective, providing a scientific basis for biochar's role in soil fertility improvement, GHG mitigation, and rice yield enhancement.

2. Materials and methods

2.1. Test site and materials

This experiment was conducted at the Shenyang Agricultural University Rice Research Institute (123°34'38.82'E, 41°49'34.15'N) and was based on a long-term biochar positioning trial initiated in 2016. The area has a temperate continental monsoon climate, the soil is brown loam with medium fertility, and the terrain is flat. Sampling was conducted in 2023. Prior to biochar application,

Journal Pre-proof

the soil organic matter (SOM) content was 15.35 g·kg^{-1}, the total nitrogen (TN) content was 0.96 g·kg^{-1}, the available nitrogen content was 63.70 mg·kg^{-1}, the available phosphorus content was 17.90 mg·kg^{-1}, the available potassium content was 70.30 mg·kg^{-1}, bulk density was 1.32 g·cm^{-3}, and the pH was 6.3. In the experiment, we used corn straw biochar, which was independently produced by the Liaoning Provincial Biochar Engineering Technology Research Centre and was prepared at 400 ℃. The basic physical and chemical properties were TN content 6.40 g·kg^{-1}, total carbon (TC) content 274.4 g·kg^{-1}, alkali-hydrolysed nitrogen content 110 mg·kg^{-1}, available phosphorus content 780 mg·kg^{-1}, available potassium content 20.9 g·kg^{-1}, electrical conductivity (EC) 17.9 m·S·cm^{-1}, and pH 9.90. The tested fertilisers were urea (46%, N), superphosphate (12%, P_2O_5), and potassium chloride (60%, K_2O).

The test rice variety was Beigeng 1501, which was provided by the Rice Research Institute of Shenyang Agricultural University. This variety has thick stems, developed roots, a compact plant type, and spindle-shaped and erect panicles, which are convenient characteristics for GHG monitoring.

2.2. Experimental design

The experiment was conducted in a completely randomised block design with biochar applied to paddy fields in April 2016 (FB) and April 2023 (NB) in the experimental treatments. Biochar was applied at 0 t·ha^{-1}, 15 t·ha^{-1}, and 45 t·ha^{-1}, respectively. The treatments were: (i) FB15, 15 t·ha^{-1} biochar applied in April 2016, (ii) FB45, 45 t·ha^{-1} biochar applied in April 2016, (iii) NB15, 15 t·ha^{-1} biochar applied in April 2023, and (iv) NB45, 45 t·ha^{-1} biochar applied in April 2023, (v) CK, no biochar applied as a control treatment, totalling five treatments with three replications. Chemical fertiliser was applied using a simple and efficient application mode. For the nitrogen fertiliser base-tillering fertiliser, panicle fertiliser was applied in a 6:4 mode, and the amount was 210 kg·ha^{-1}. For potassium fertiliser application as a base fertiliser, panicle fertiliser was applied in a 5:5 mode, and phosphorus fertiliser was applied once as a base fertiliser. The amount of phosphorus and potassium fertiliser was 180 kg·ha^{-1}. The plot area was 3.0 × 3.3 m, with a total of 15 plots. A black hard plastic baffle was used in each plot as a wall to a subsurface depth of 25 cm to prevent the string of water and fertiliser. Other management measures were conducted in accordance with conventional high-yield cultivation.

2.3. Sample collection and analysis

For gas collection, we adopted the static dark box method, whereby the box was completely wrapped in heat-insulated aluminium foil to continuously monitor GHGs in the paddy field. The length, width, and height of the dark box were 0.5 m, 0.3 m, and 0.7 m, respectively. When the rice plant height exceeded that of the dark box, a two-way open dark box with a height of 0.3 m was added on the lower side. To make the gas in the box uniform, a 12-V fan driven by a battery was

Journal Pre-proof

installed inside the top of the dark box. A dark box base with a groove was placed in each plot (the height was consistent with the ground) to inject water into the groove to seal the box before gas collection. GHG collection was carried out on the fifth day after rice transplanting. Greenhouse gas samples were collected between 08:00 and 11:00 a.m. throughout the entire rice growth period under rainless conditions. Sampling was conducted every 7 days, with an additional collection 3 days after fertilisation. During gas collection, a 50-mL syringe was used to pump back and forth at 0, 10, 20, and 30 min; gas was extracted and stored in an aluminium foil vacuum gas collection bag (0.1 L), and the temperature in the box was measured. Gas samples were transported to the laboratory to determine CH_4 concentrations using a GHG analyser (Agilent 7890B18001268S) equipped with a hydrogen ionisation detector.

The calculation formula of the CH_4 emission flux is as follows (Li et al., 2015a):

$$F = \rho \times V/A \times dc/dt \times 273/(273 + T)$$

where F is the CH_4 emission flux ($mg \cdot m^{-2} \cdot h^{-1}$ or $\mu g \cdot m^{-2} \cdot h^{-1}$); ρ is the CH_4-C density in the standard state (0.54 g/L); v is the effective volume (m^3) in the sampling box; A is the soil surface area (m^2) covered by the sampling box; dc/dt is the CH_4 emission rate ($\mu L \cdot L^{-1} \cdot h^{-1}$]); t is the average temperature (°C) in the static chamber during sampling.

The formula for calculating the total cumulative CH_4 emissions is as follows (Wang et al., 2024):

$$T = \sum \frac{F_{i+1} + F_i}{2} \times D_{i+1} - D_i \times 24$$

where T is the total CH_4 emission ($kg \cdot ha^{-1}$), F_i and F_{i+1} are the average CH_4 emission fluxes ($mg \cdot m^{-2} \cdot h^{-1}$) at the ith and i+1 times of sampling, respectively, and D_{i+1} and Di are the ith and i+1 sampling times (d), respectively. Total CH_4 emissions were calculated as the average of four repeated observations weighted by the time interval.

At the rice heading stage, the five-point sampling method was used to collect soil samples from each plot. Under flooded conditions, soil from the 0–20 cm layer was extracted using a soil auger and thoroughly mixed to ensure homogeneity. Samples were collected in sterile plastic bags, immediately transported to the laboratory in dry ice, and stored in a –80 °C ultra-low temperature refrigerator for subsequent DNA extraction.

2.4. Fluorescence quantitative qPCR

Quantitative polymerase chain reaction (qPCR) was performed using a real-time fluorescent qPCR instrument (Applied Biosystems, USA). The quantitative PCR reagent used was ChamQ SYBR Color qPCR Master Mix (2X), which was provided by Nanjing Novozymes Biotechnology Co., Ltd.

The key methanogen and methanotroph genes *mcrA* and *pmoA* were quantitatively analysed. The specific primers mcrA-F (5′-GGTGGTGTMGGATTCACACARTAYGCWACAGC-3′) and

Journal Pre-proof

mcrA-R (5′-TTCATTGCRTAGTTWGGRTAGTT-3′) were used to amplify the *mcrA* gene of methanogens. The specific primers A189F (5′-GGNGACTGGGACTTCTGG-3′) and mb661R (5′-CCGGMGCAACGTCYTTACC-3′) were used to amplify the *pmoA* gene of methanotrophs. Each sample was tested thrice in parallel, and the average value was calculated.

2.5. Metagenomic analysis

2.5.1. Sample DNA extraction

Samples were transported to Shanghai Meiji Biomedical Technology Co., Ltd. for DNA extraction and Illumina sequencing. First, DNA was extracted using an MJ-Feces soil DNA kit, and the DNA purity and concentration were detected using a NanoDrop2000 and TBS-380. DNA integrity was detected by 1% agarose gel electrophoresis. DNA was disrupted into a fragment of approximately 350 bp by Covaris M220, which was used to construct a PE library.

2.5.2. Library construction and Illumina sequencing

A NEXTFLEX® Rapid DNA-Seq Kit was used to construct the library. First, the adaptor self-ligation fragments were removed by magnetic bead screening. Secondly, PCR amplification was used to enrich the library template. Finally, the PCR products were recovered by magnetic beads to obtain the final library. Metagenomic sequencing was performed using the Illumina NovaSeq sequencing platform (Shanghai Meiji Biomedical Technology Co., Ltd.). First, one end of the library molecule was complementary to the primer base. After one round of amplification, the template information was fixed on the chip. The other end of the fixed molecule was randomly complementary to another nearby primer and was also fixed to form a bridge. Secondly, PCR amplification was carried out to produce DNA clusters. After the DNA amplicon was linearised into a single strand, the modified DNA polymerase and dNTP with four fluorescent markers were added, and only one base was synthesised in each cycle. The reaction plate surface was scanned by a laser, and the types of nucleotides polymerised by the first round of reaction of each template sequence were read. The fluorescent group and termination group were chemically cleaved to restore the 3′-end reactivity, allowing polymerisation of the next nucleotide to continue. Finally, the sequence of the template DNA fragment was determined by analysing the fluorescence signal data collected in each cycle.

2.5.3. Analysis

Fastp software (Chen et al., 2018) was used to remove reads with a length of < 50 bp, an average base mass value of < 20, and N-containing bases, and to retain high-quality pair-end and single-end reads. The assembly software MEGAHIT (Li et al., 2015), based on the principle of concise de Bruijn graphs, was used to assemble the optimised sequences, and contigs ≥ 300 bp were selected as the final assembly results. Prodigal (Hyatt et al., 2010)/MetaGene (Noguchi et al., 2006)

Journal Pre-proof

was used to predict the open reading frame of contigs in the splicing results. Genes with nucleic acid length ≥ 100 bp were selected and translated into amino acid sequences.

CD-HIT (Fu et al., 2012) was used to cluster the predicted gene sequences of all samples (parameters: 90% identity, 90% coverage) to construct a non-redundant gene set. Using SOAPaligner (Li et al., 2008) software, high-quality reads of each sample were compared with non-redundant gene sets (95% identity), and abundance information of genes in the corresponding samples was counted. Diamond (Buchfink et al., 2015) was used to compare the amino acid sequences of non-redundant gene sets with NR, KEGG, and COG databases (the BLASTP comparison parameter setting expectation e-value is $1e^{-5}$), to obtain species and functional annotation information regarding genes and functional and species abundance based on gene set abundance.

2.6. Data processing

Microsoft Excel 2022 was used for data collation, a one-way analysis of variance was performed using IBM SPSS Statistics 27.0.1, and the GHG emission flux was plotted using Origin 2022. Metagenomic sequencing data were visualised using the Meiji cloud platform, and mapping was performed using the R language.

3. Results and analysis

3.1. Soil properties

Biochar changed the physicochemical soil properties during the study period (Table 1). The SOM level varied between treatments throughout the rice tillering stage; NB45 exhibited the highest SOM content, which was significantly different from that of CK. However, no significant difference was seen between the SOM content in CK and that in FB15 and NB15. Compared to CK, the TC content of FB15, NB15, and NB45 increased by 20.08%, 32.89%, and 71.11%, respectively ($P < 0.05$), and the TN content increased by 16.48%, 24.18%, and 37.36% ($P < 0.05$), respectively. The TC and TN contents of FB45 exceeded those of CK, though the difference was not statistically significant. The application of biochar resulted in an increase in soil pH. In comparison to CK, the relationship between the increase in soil pH across treatments diminished in the following order: NB45 (17.08%) > FB45 (3.50%) > FB15 (2.48%) > NB15 (2.04%). The SOM contents of NB15 and NB45 were significantly different from CK at the heading stage (Table 1), being 1.35 and 1.64 times higher than CK, respectively. The TC content of each treatment differed significantly compared to CK, with a decreasing order: NB45 (58.68%) > FB45 (34.90%) > NB15 (30.09%) > FB15 (11.94%). The TN content exhibited a decreasing trend: NB45 (26.60%) > NB15 (14.90%) > FB45 (10.64%) > FB15 (2.13%), with no significant difference between FB15 and CK. Compared with CK, the pH of FB45, NB15, and NB45 increased significantly by 11.52%, 4.60%, and 3.99%,

Journal Pre-proof

respectively. The pH of FB15 was higher than that of CK but the difference was not significant. At the rice maturity stage, the SOM content of NB45 remained the highest (78.40 g·kg^{-1}). The SOM content in all treatments differed significantly from that of CK, exhibiting a decrease in the order of NB45 > NB15 > FB45 > FB15. The TC and TN contents of CK were the lowest and exhibited significant differences compared to other treatments. The content order was NB45 > NB15 > FB45 > FB15. The pH of NB45, NB15, and FB45 increased significantly by 18.31%, 9.67%, and 6.04%, respectively, compared to CK.

Table 1

Effect of years of biochar application on soil physicochemical properties of rice at three periods of growth

Period	Treatment	SOM (g·kg^{-1})	TC (g·kg^{-1})	TN (g·kg^{-1})	pH
Tillering stage	CK	55.75 ± 3.76c	9.76 ± 0.68d	0.91 ± 0.01c	6.85 ± 0.05d
	FB15	57.46 ± 2.58bc	11.72 ± 0.08c	1.06 ± 0.07b	7.02 ± 0.03bc
	FB45	43.92 ± 6.01c	10.69 ± 0.03d	0.95 ± 0.01c	7.09 ± 0.02b
	NB15	58.14 ± 2.42bc	12.97 ± 0.38b	1.13 ± 0.00b	6.99 ± 0.05c
	NB45	71.46 ± 15.07a	16.70 ± 0.26a	1.25 ± 0.00a	8.02 ± 0.03a
Ear sprouting period	CK	42.56 ± 1.88c	9.97 ± 0.16d	0.94 ± 0.01d	6.77 ± 0.02c
	FB15	45.29 ± 3.78bc	11.16 ± 0.46c	0.96 ± 0.02d	6.83 ± 0.02c
	FB45	52.80 ± 1.20abc	13.45 ± 0.16b	1.04 ± 0.00c	7.04 ± 0.04b
	NB15	57.35 ± 5.12ab	12.97 ± 0.19b	1.08 ± 0.01b	7.08 ± 0.02b
	NB45	63.95 ± 14.68a	15.82 ± 0.42a	1.19 ± 0.01a	7.55 ± 0.05a
Maturity	CK	50.98 ± 2.27d	11.48 ± 0.05d	1.06 ± 0.01d	5.79 ± 0.02d
	FB15	59.40 ± 1.02c	13.97 ± 0.26c	1.17 ± 0.04c	5.84 ± 0.03d
	FB45	61.10 ± 2.39c	14.68 ± 0.84c	1.28 ± 0.05b	6.14 ± 0.03c
	NB15	70.66 ± 5.82b	16.55 ± 0.01b	1.31 ± 0.03b	6.35 ± 0.03b
	NB45	78.40 ± 3.65a	22.14 ± 1.13a	1.51 ± 0.03a	6.85 ± 0.03a

Note: Data are mean values ± standard deviation. Different lowercase letters in the same column indicate a significant difference ($P < 0.05$). CK: no biochar application; FB15 and FB45: eighth year of biochar treatment with application rates of 15 and 45 t·ha^{-1}, respectively; NB15 and NB45: first year of biochar treatment with application rates of 15 and 45 t·ha^{-1}, respectively.

3.2. CH$_4$ emissions from paddy fields

As shown in Fig. 1a, the CH$_4$ emission fluxes from paddy soils under different scenarios of biochar application durations followed a similar trend. Monitoring of CH$_4$ emissions commenced 5 days after transplanting, with the first peaks observed in NB15 and NB45 following the initial fertiliser application. The highest flux was recorded in NB45, reaching 116.76 mg·m^{-2}·h^{-1}, after which emissions exhibited a declining trend. Following the second fertiliser application, NB15 exhibited the highest peak of the entire growth cycle, reaching 107.60 mg·m^{-2}·h^{-1}. After the third

Journal Pre-proof

fertiliser application, all treatments displayed an emission peak, with the emission fluxes following a distinct pattern: NB15 (102.27 $mg{\cdot}m^{-2}{\cdot}h^{-1}$) > NB45 (75.53 $mg{\cdot}m^{-2}{\cdot}h^{-1}$) > CK (50.11 $mg{\cdot}m^{-2}{\cdot}h^{-1}$) > FB15 (27.73 $mg{\cdot}m^{-2}{\cdot}h^{-1}$) > FB45 (15.93 $mg{\cdot}m^{-2}{\cdot}h^{-1}$). Subsequently, all treatments exhibited a gradual decline in CH_4 emissions. The emission fluxes of CK, FB15, and FB45 followed a similar trend throughout the reproductive stage, initially increasing slowly before gradually decreasing. In contrast, NB15 and NB45 exhibited two distinct emission peaks during the growth cycle. From approximately 35 days after transplanting, the emission fluxes of NB45 were consistently lower than those of NB15. The overall emission trend throughout the experiment was as follows: NB15 > NB45 > CK > FB15 > FB45.

Compared with CK, cumulative CH_4 emissions increased significantly in NB15 and NB45 (NB15 > NB45). In contrast, CH_4 emissions in FB15 and FB45 were significantly lower than in CK (FB15 > FB45).

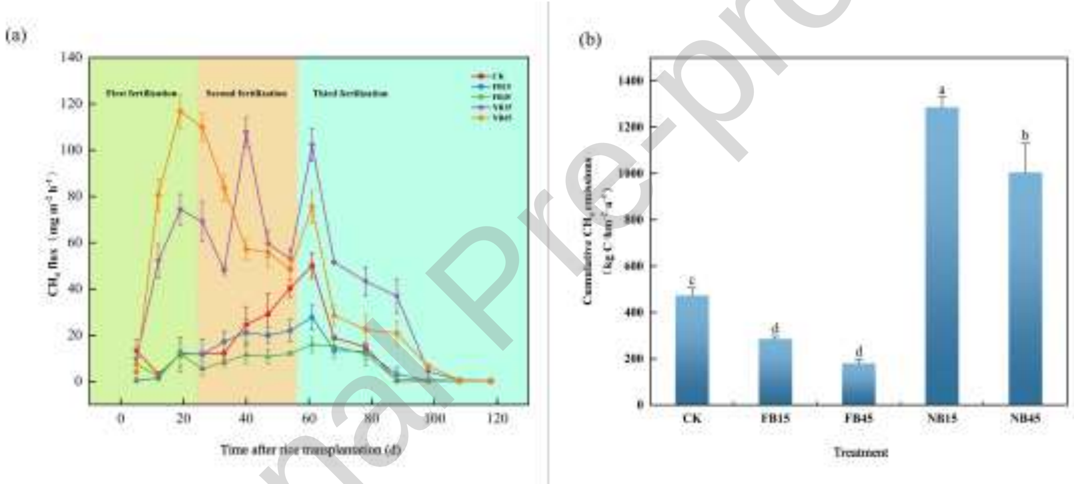

Fig. 1. (a) CH_4 flux and (b) cumulative CH_4 emissions under different biochar application durations. Error bars represent the standard error (n = 3), and different lowercase letters indicate significant differences between treatments ($P < 0.05$). CK: no biochar application; FB15 and FB45: eighth year of biochar treatment with application rates of 15 and 45 $t{\cdot}ha^{-1}$, respectively; NB15 and NB45: first year of biochar treatment with application rates of 15 and 45 $t{\cdot}ha^{-1}$, respectively.

3.3. Production analysis

Rice yields under biochar treatments were significantly higher than those in CK (Table 2). There was no significant difference in 1000-grain weight or effective panicle number between treatments with different biochar application durations and CK. When comparing the number of grains per panicle across biochar application durations, a decreasing trend was observed: NB15 > FB15 and FB45 > NB45, with all biochar treatments showing higher values than CK. A similar pattern was observed for the seed setting rate, which also followed the trend NB15 > FB15 and FB45 > NB45, with all biochar treatments exceeding CK. Compared with CK, the theoretical yields of FB15, NB15, FB45, and NB45 increased significantly by 13.50%, 9.27%, 14.68%, and 12.58%,

Journal Pre-proof

respectively. At the same application duration, theoretical yield followed the trend FB45 > FB15 and NB45 > NB15, indicating an increasing trend with higher biochar application rates.

Table 2

Effect of biochar application duration and amount on rice yields and yield components

Treatment	1000-grain weight (g)	Effective panicles (m^2)	Grain number per panicle	Seed setting rate (%)	Theoretical yield ($t \cdot ha^{-1}$)
CK	24.30 ± 0.40a	250.00 ± 25.00a	168.44 ± 1.18b	87.40 ± 0.08ab	9.06 ± 0.07b
FB15	24.77 ± 0.47a	283.33 ± 14.43a	158.97 ± 0.99c	92.28 ± 1.67a	10.28 ± 0.31a
FB45	24.72 ± 0.22a	266.67 ± 14.33a	176.06 ± 2.35a	91.92 ± 1.68a	10.39 ± 0.37a
NB15	24.59 ± 0.86a	258.33 ± 28.86a	177.82 ± 2.45a	86.50 ± 2.24b	9.90 ± 0.01a
NB45	24.48 ± 0.15a	258.33 ± 14.43a	171.34 ± 0.10b	89.11 ± 4.31ab	10.20 ± 0.10a

Note: Data are mean values ± standard deviation. Different lowercase letters in the same column indicate a significant difference between treatments ($P < 0.05$). CK: no biochar application; FB15 and FB45: eighth year of biochar treatment with application rates of 15 and 45 $t \cdot ha^{-1}$, respectively; NB15 and NB45: first year of biochar treatment with application rates of 15 and 45 $t \cdot ha^{-1}$, respectively.

3.4. Real-time fluorescent quantitative qPCR

Copy numbers of *pmoA* and *mcrA* genes in soil treated with biochar at the rice heading stage were higher than those in CK (Fig. 2). The results showed that biochar application in the eighth year continued to increase the *pmoA* gene abundance in paddy soil. The copy number of the FB45 gene was higher than that of FB15 and CK; however, the difference was not obvious. Biochar application in the first year had a greater impact on *pmoA* gene abundance. Gene copy numbers of NB15 and NB45 were significantly higher by 114.95% and 88.62%, respectively, and those of FB15 and FB45 were 24.37% and 58.19% higher, respectively, compared to those of CK. Gene abundance decreased in the following order: NB15 > NB45 > FB45 > FB15 > CK. The copy number of the *mcrA* gene in the soil of NB15 and NB45 treatments was significantly higher than that of other treatments; there was no significant difference between NB15 and NB45. The *mcrA* gene abundance was the lowest in CK, and FB15 and FB45 gene abundance was 2.23 and 2.70 times higher than that of CK, respectively. The *pmoA/mcrA* ratio decreased in the following order: CK > FB45 > FB15 > NB45 > NB15; it was significantly higher in CK than in biochar treatments. The *pmoA/mcrA* ratio was similar between FB15 and FB45 and between NB15 and NB45.

Journal Pre-proof

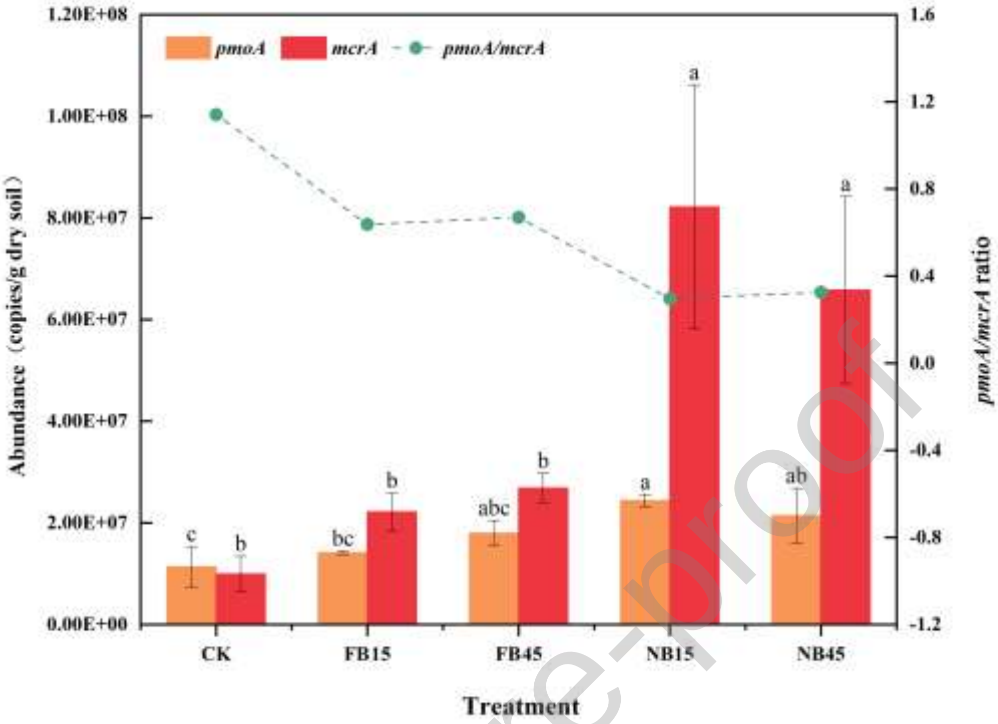

Fig. 2. Copy numbers of the *pmoA* and *mcrA* genes and *pmoA/mcrA* ratios of soils under biochar treatments at the rice heading stage. Different capital and lowercase letters indicate a significant difference ($P < 0.05$) between treatments in the logarithm of *pmoA* and *mcrA* gene copy numbers. CK: no biochar application; FB15 and FB45: eighth year of biochar treatment with application rates of 15 and 45 t·ha^{-1}, respectively; NB15 and NB45: first year of biochar treatment with application rates of 15 and 45 t·ha^{-1}, respectively.

3.5. Metagenomic sequencing analysis of methanogens and methanotrophs

3.5.1. Analysis of methanogen and methanotroph communities

The community composition abundance at the genus level of methanogens (Fig. 3a) was determined, and the dominant flora *Chloroflexota* (Fig. 3b), *Deltaproteobacteria* (Fig. 3c), *Anaerolineales* (Fig. 3d), and *Methanosarcina* (Fig. 3e) were compared. *Chloroflexota* abundance accounted for the largest proportion in all treatments, and its richness was the highest in FB15 (22.85%). Compared with CK, NB15 and NB45 were significantly lower, and the difference was extremely significant ($P < 0.001$). There was no significant difference among FB15, FB45, and CK. Under FB and NB conditions, there was no significant difference between different biochar application rates. *Deltaproteobacteria* abundance was only lower than that of *Chloroflexota*, and the proportion was similar in each treatment, accounting for 8.85% in CK, 8.80% in FB15, 8.10% in FB45, 7.87% in NB15, and 9.23% in NB45. The difference between NB15 and NB45 was significant ($P < 0.05$). *Anaerolineales* abundance in each treatment was relatively low; compared

Journal Pre-proof

with CK (4.88%), FB15 (5.79%), and FB45 (6.26%), the richness of NB15 (4.52%) and NB45 (3.86%) was significantly lower. The richness of FB15 and FB45 was higher than that of CK, and that of FB45 was significantly higher than that of CK. Under FB and NB conditions, there was no significant difference between different biochar application rates. *Methanosarcina* abundance differed significantly between treatments (Fig. 3a). The NB15 (4.52%) and NB45 (2.94%) abundances were significantly higher than those of other treatments, and there was a significant difference between NB15 and NB45 ($P < 0.05$). These treatments were compared with CK (0.94%), FB15 (1.32%), and FB45 (1.47%), showing significant differences. However, there was no significant difference among CK, FB15, and FB45.

The community composition abundance at the genus level of methanotrophs (Fig. 3f) was determined, and the dominant flora *Chloroflexota* (Fig. 3g), *Deltaproteobacteria* (Fig. 3h), *Acidobacteriota* (Fig. 3i), and *Anaerolineales* (Fig. 3j) were compared in multiple groups. The largest proportion of abundance in all treatments was that of *Chloroflexota*. Compared with CK (16.83), FB15 (17.69%), and FB45 (16.21%), the abundance of NB15 (12.93%) and NB45 (13.30%) was significantly lower, showing significant differences. In contrast, the abundance of FB15 and FB45 was similar to that of CK. Under FB and NB conditions, there was no significant difference between different biochar application rates. *Deltaproteobacteria* abundance in each treatment was similar, ranging from 9.96% to 11.15%. *Acidobacteriota* richness was highest in CK (7.62%) and lowest in NB45 (4.82%). There were significant differences in *Acidobacteriota* richness between CK and other treatments. A comparison of FB15 and FB45 with NB15 and NB45, respectively, showed significant differences; however, there was no significant difference between different biochar application rates under FB and NB conditions. *Anaerolineales* abundance was compared in different treatments. There was still no significant difference between different biochar application rates under FB and NB conditions. NB15, NB45, and FB45 showed significant differences compared with CK.

Journal Pre-proof

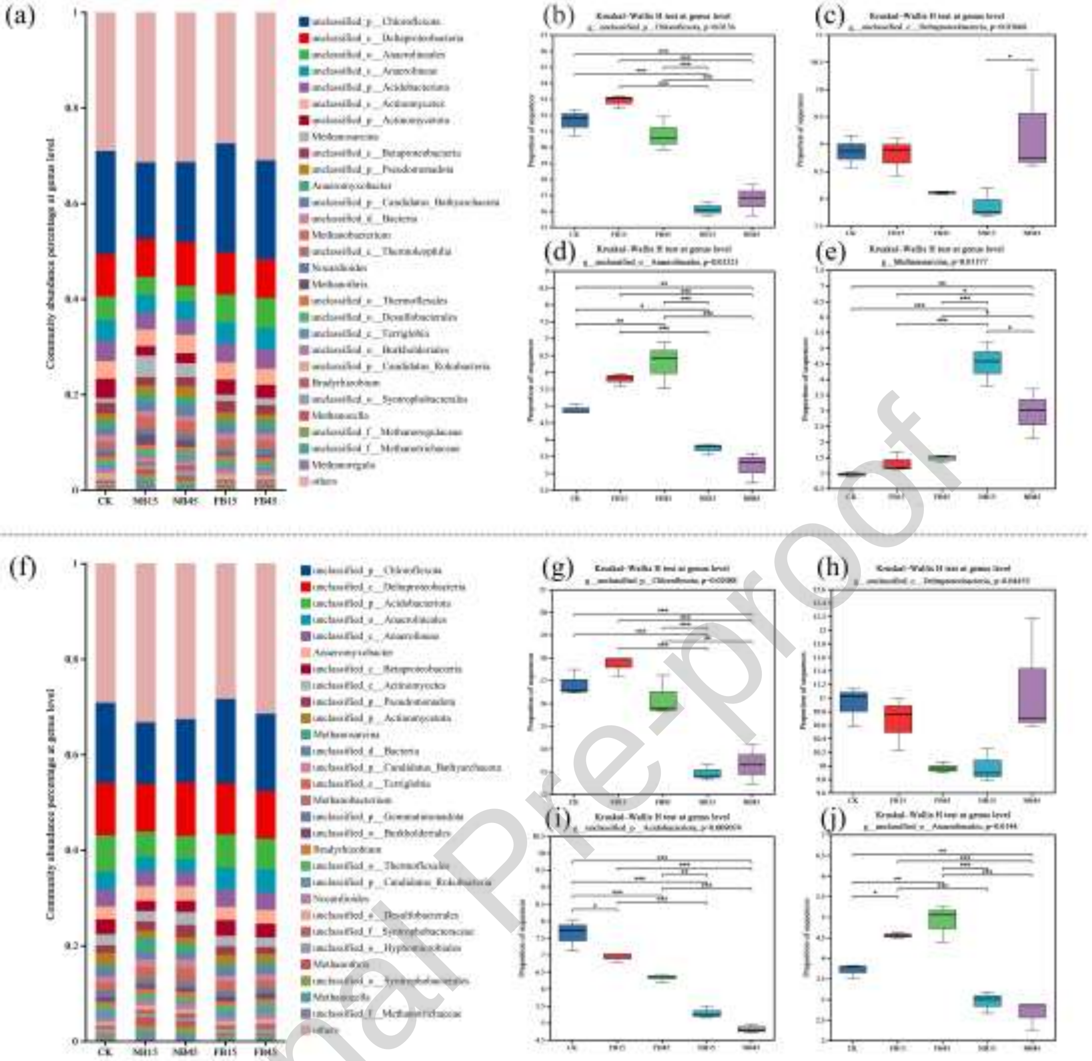

Fig. 3. Microbial community composition at the genus level of methanogenic (a) and methane-oxidising (f) bacteria. Comparison of intergroup differences in *Chloroflexota/Deltaproteobacteria/Anaerolineales/Methanosarcina* between methanogenic (b, c, d, e) and methane-oxidising (g, h, I, j) bacteria. CK: no biochar application; FB15 and FB45: eighth year of biochar treatment with application rates of 15 and 45 t·ha^{-1}, respectively; NB15 and NB45: first year of biochar treatment with application rates of 15 and 45 t·ha^{-1}, respectively.

3.5.2. Functional analysis of methanogens and methanotrophs

The KEGG database was used to classify the top 50 methanogens and perform functional and cluster analyses. A total of 11 functional pathways were detected (Fig. 4a). The metabolic functions of all treated methanogens were mainly concentrated in carbon metabolism, *Microbial metabolism in diverse environments, Metabolic pathways,* and *Methane metabolism*. The metabolic functions of all treated methanotrophs (Fig. 4b) mainly focused on *Glyoxylate and dicarboxylate metabolism, Carbon metabolism, Microbial metabolism in diverse environments, Metabolic pathways,* and *Methane metabolism*. According to the cluster analysis, the hierarchical relationship between

Journal Pre-proof

methanogens and methanotrophs was consistent. In the first level, the metabolic functions of methanogens and methanotrophs in NB15 and NB45 were highly similar, and those of CK and FB15 were similar. In the second level, FB45 had higher similarity with CK and FB15. In the third level, NB15 and NB45 had lower similarity with metabolic functions in other treatments.

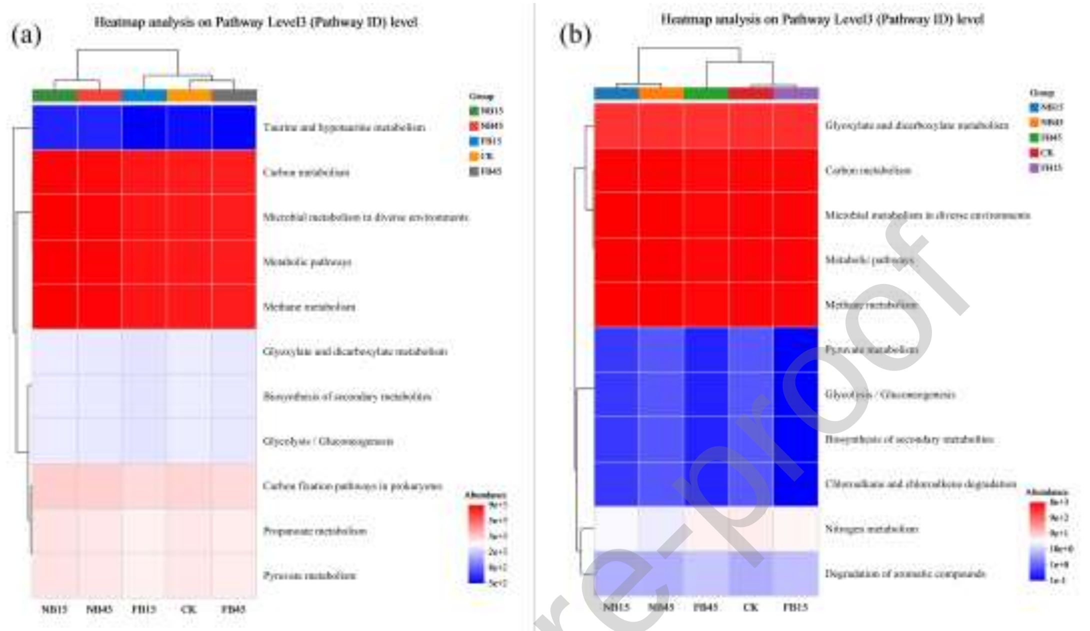

Fig. 4. Metabolic function and cluster analysis of (a) methanogens and (b) methanotrophs. CK: no biochar application; FB15 and FB45: eighth year of biochar treatment with application rates of 15 and 45 t·ha^{-1}, respectively; NB15 and NB45: first year of biochar treatment with application rates of 15 and 45 t·ha^{-1}, respectively.

3.5.3. Function comparison and difference analysis of methanogens and methanotrophs

PCoA analysis and ANOSIM analysis were performed on methanogens and methanotrophs in all treatments (Fig. 5). Functional differences of methanogens in all treatments were significantly greater between groups than within groups (ANOSIM: R = 0.767407, P = 0.001) (Fig. 5b). PCoA analysis results (Fig. 5a) showed that the functional similarity of methanogens could be divided into three groups according to the aggregation degree. The functional effects of NB15 and NB45 and of FB45 and CK were relatively close. Compared with CK, FB15, and FB45, the functional similarity of NB15 and NB45 was significantly different, and the similarity of FB15 was lower than that of other treatments. Functional differences of methanotrophs in all treatments were significantly greater between groups than within groups (ANOSIM: R = 0.810370, P = 0.001) (Fig. 5d), as determined by PCoA (Fig. 5c). The functional similarity of methanotrophs could be divided into three groups according to the aggregation degree. The results showed that functional similarity was high between NB15 and NB45 and between FB15 and CK. NB15 and NB45 were compared with the other three groups, and the similarity was different. The functional similarity of methanotrophs

Journal Pre-proof

in FB45 differed significantly from that in other treatments.

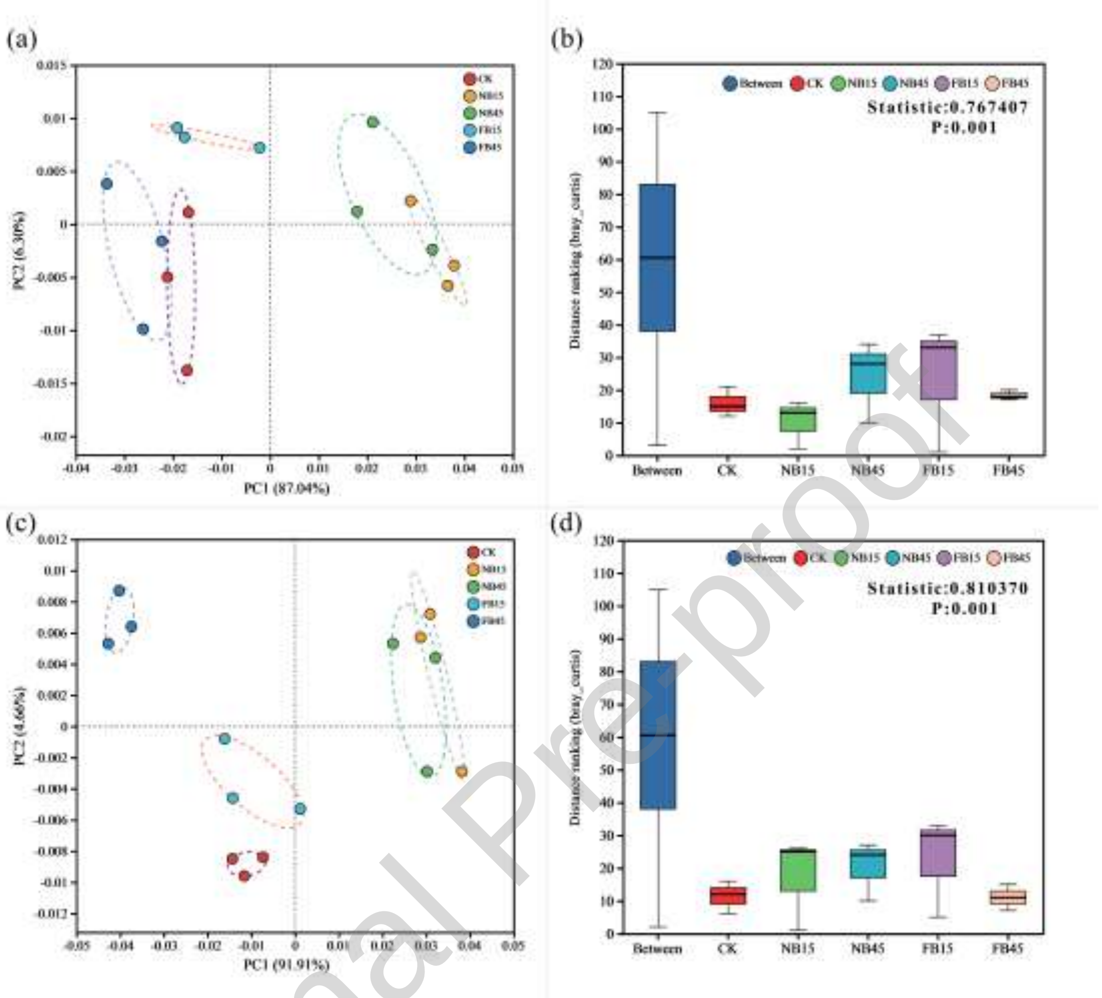

Fig. 5. Comparative analysis of PCoA function of (a) methanogens and (c) methanotrophs. ANOSIM analysis of (b) methanogens and (d) methanotrophs. CK: no biochar application; FB15 and FB45: eighth year of biochar treatment with application rates of 15 and 45 t·ha^{-1}, respectively; NB15 and NB45: first year of biochar treatment with application rates of 15 and 45 t·ha^{-1}, respectively.

3.5.4. Differential analysis of CH_4 metabolic function between methanogens and methanotrophs

The CH_4 metabolic pathways involved in the metabolic functions of methanogens and methanotrophs were analysed to determine individual group differences. Under different treatments, methanogens involved in CH_4 metabolism exhibited significant differences (Fig. 6a). Significant differences were observed between FB45 and NB45 and between CK and FB15 ($P < 0.05$). Additionally, there was a significant difference between CK and NB45 ($P < 0.01$), while the difference between NB15 and CK was highly significant ($P < 0.001$). Similarly, CH_4-oxidising bacteria involved in CH_4 metabolism also showed statistically significant differences across treatments (Fig. 6b). The difference between FB15 and CK was significant ($P < 0.05$). The CH_4 metabolic function in NB15 and NB45 treatments differed significantly from that in CK ($P < 0.001$).

Journal Pre-proof

The CH_4 metabolic function of FB15, NB15, and NB45 differed significantly from that of FB45 ($P < 0.001$).

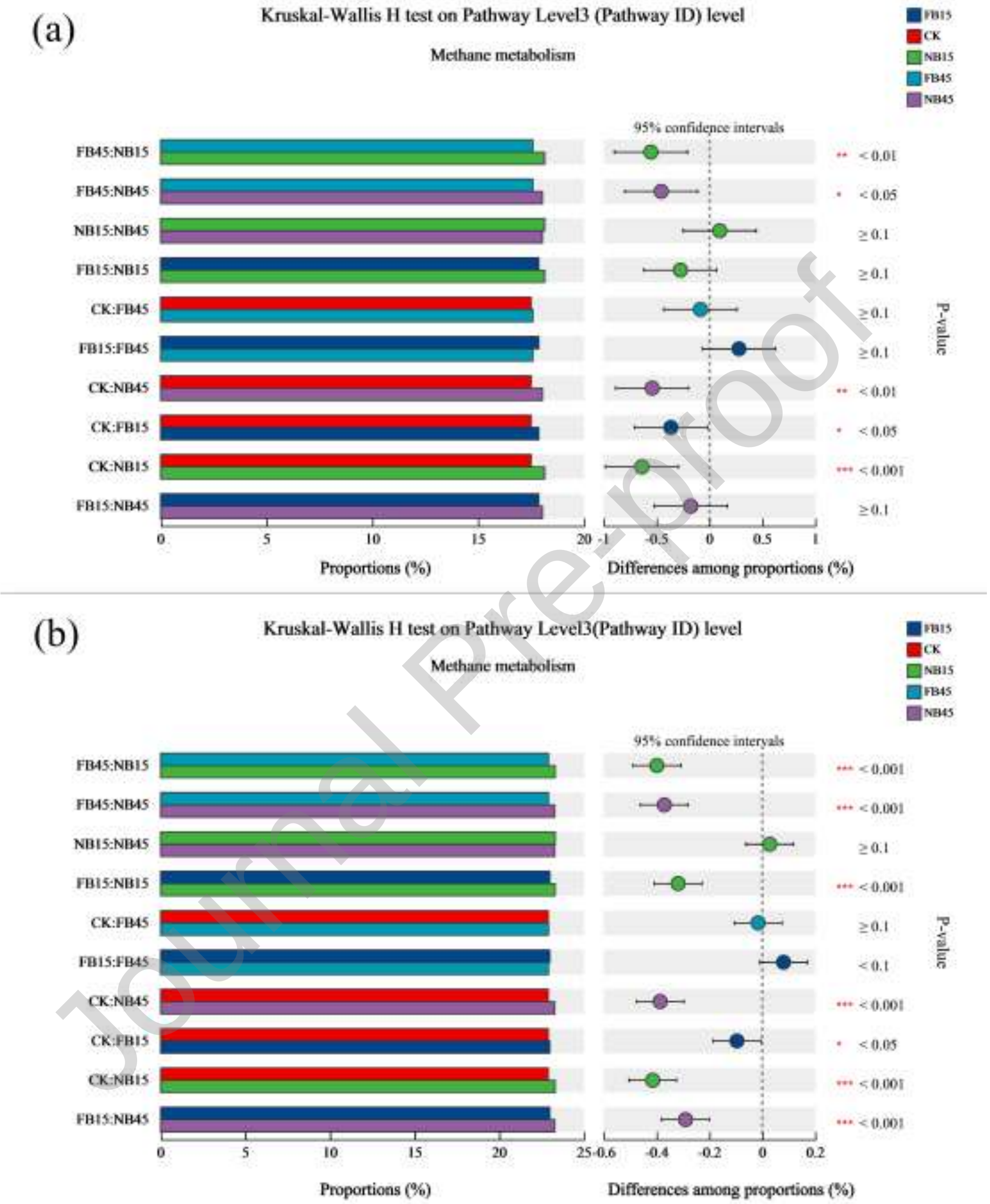

Fig. 6. Intergroup comparisons of methane metabolism functions of methanogenic (a) and methane oxidising (b) bacteria. CK: no biochar application; FB15 and FB45: eighth year of biochar treatment with application rates of 15 and 45 t·ha^{-1}, respectively; NB15 and NB45: first year of biochar treatment with application rates of 15 and 45 t·ha^{-1}, respectively.

3.6. Analysis of the correlation between environmental factors affecting methanogens and

Journal Pre-proof

methanotrophs

Redundancy analysis (RDA) of the methanogen community and environmental factors (Fig. 7a) showed that the cumulative contribution of the first two ordination axes reached 75.62%, and there was a positive correlation among all environmental factors. Among them, TN had the greatest effect on species community composition ($P = 0.002$, $r^2 = 0.64408$), followed by pH ($P = 0.005$, $r^2 = 0.54813$). All environmental factors were positively correlated with NB15 and NB45 and had similar effects on the other three groups. RDA analysis of methanotrophs (Fig. 7b) showed that the cumulative contribution rate reached 74.48%, and there was a positive correlation between all environmental factors. Among them, TN had the greatest effect on species community composition ($P = 0.001$, $r^2 = 0.69651$), followed by pH ($P = 0.004$, $r^2 = 0.60413$). There was a positive correlation between all environmental factors and NB15 and NB45, and the degree of the effect on the other three groups was similar.

The correlation between environmental factors and methanogenic function was determined by Mental test analysis (Fig. 7c). The methanogenic function of FB45 had a significantly positive correlation with TN ($P < 0.001$) and a positive correlation with SOM ($P \geq 0.05$). NB45 was positively correlated with pH ($P \geq 0.05$). CK was positively correlated with SOM and pH ($P \geq 0.05$). NB15 was positively correlated with TC, C/N, and TN ($P \geq 0.05$). FB15 was positively correlated with TC, SOM, TN, and C/N ($P \geq 0.05$). The Mental test analysis of methanotroph function and environmental factors (Fig. 7d) showed that the methanotroph function of FB45 was positively correlated with TN ($P < 0.001$), TC, and C/N ($0.001 < P < 0.05$); FB15 was positively correlated with TN, TC, SOM, and C/N ($P \geq 0.05$); CK was positively correlated with pH and SOM ($P \geq 0.05$); NB15 was negatively correlated with all environmental factors ($P \geq 0.05$); and NB45 was positively correlated with SOM ($P \geq 0.05$).

Journal Pre-proof

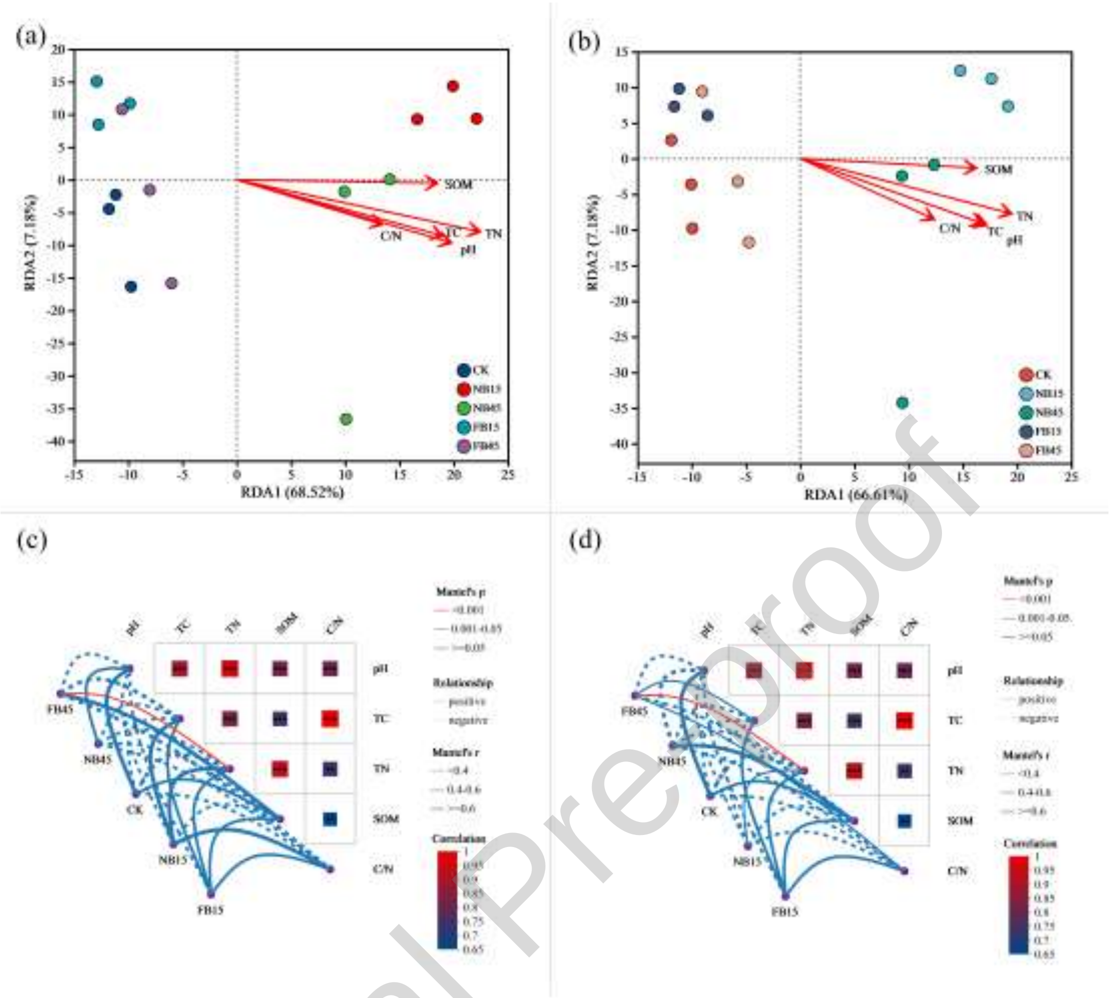

Fig. 7. RDA analysis of environmental factors and community composition of (a) methanogens and (b) methanotrophs across biochar treatments. Functional RDA analysis of (c) methanogens and (d) methanotrophs between environmental factors and treatments. CK: no biochar application; FB15 and FB45: eighth year of biochar treatment with application rates of 15 and 45 t·ha^{-1}, respectively; NB15 and NB45: first year of biochar treatment with application rates of 15 and 45 t·ha^{-1}, respectively.

Journal Pre-proof

4. Discussion

4.1. Effects of biochar application duration on paddy soil properties

Biochar application positively affects improvements in soil physical and chemical properties in paddy fields (Wang et al., 2024). In the present study, the SOM content changed significantly in the three periods of the rice growing season. Biochar application significantly increased the SOM content in the soil, which was consistent with the results of biochar application in double-cropping rice paddy soil (Li et al., 2023). Regarding the effect of different biochar application durations on SOM, the results of this study suggest that the first year of biochar application had a greater effect on SOM, and that the effect changed with the amount of biochar applied, in agreement with previous research (Liu et al., 2024). The findings of this study showed that when the application period reached 8 years, biochar continued to increase SOM, which was related to the amount of biochar applied. It has been shown that biochar application can increase soil TN and TC, whereas soil TN and TC content increase with an increase of biochar application (Jin et al., 2024; Luo et al., 2017; Singla et al., 2014), a finding that is consistent with the results of this study. The high porosity, high internal surface area, and large number of micropores of biochar may potentially improve soil physicochemical properties (Ali et al., 2021); however, there is a lack of research on the effect of biochar application duration. Apostolović et al., (2024) reported significant reductions in soil TC levels under long-term impacts compared to short-term impacts of biochar. The present study showed that the TN and TC contents in paddy soil continued to increase in the eighth year of biochar application. It may be related to the different biochar types and biochar action times we observed, which need to be further investigated in depth. pH is an important soil property (Cao et al., 2022). A study on soil pH following field biochar aging showed that biochar application increases soil pH, with fresh biochar causing a more pronounced pH elevation than aged biochar (Wang et al., 2021). When considering biochar application rate as the only variable, it was observed that higher biochar application rates led to an increase in soil pH (Wang et al., 2024), a finding consistent with the results of the present study. This may be due to the release of a large number of cations from the alkaline bases in biochar to the soil, which increases the proton consumption process, thereby increasing the soil pH and reducing soil acidity. The higher the amount of biochar applied (within the optimal range), the higher the soil pH (Khan et al., 2024). There are also studies that suggest that biochar has no long-term effect on pH (Quilliam et al., 2013), which may be due to differences in the amount of biochar applied and settling of biochar. However, there is a lack of in-depth research under an increased biochar application duration. This study showed that the ability to increase soil pH after 8 years of biochar application was weaker than that of biochar applied in the first year.

4.2. Effects of biochar application duration on CH_4 emissions and rice yield

Previous studies have reported contradictory results regarding the effect of biochar on CH_4 emissions; some studies suggest that biochar application can reduce CH_4 emissions (Dai et al., 2024; Gao et al., 2024), while other studies present an opposing perspective (Qi et al., 2023; Liu et al., 2021). In the present study, CH_4 emissions from paddy fields were monitored during the whole growth period after rice transplanting. The results showed that CH_4 emissions increased significantly in the first year of biochar application but were alleviated in the eighth year of biochar application, thereby confirming the dual impact of biochar application on CH_4 emissions. In a previous study, CH_4 emissions were monitored for 2 years after biochar application, and the conclusion was similar to that of the present study (Feng et al., 2020). Similarly, the cumulative CH_4 emissions increased in the first year of application. In the case of the same number of application years, CH_4 emissions under a high biochar content were lower than those under a low biochar content, which is consistent with previous research (Wang et al., 2021). This may be because biochar

Journal Pre-proof

application increased SOM content, enhanced the oxidation capacity of paddy soil, and increased the activity of methane-oxidising bacteria, thereby reducing CH_4 production (Qin et al., 2016; Feng et al., 2011). In this study, the effect of biochar on CH_4 emissions was studied under long-term positioning conditions, with a focus on the temporal dynamics of biochar efficiency. The findings provide a scientific basis for understanding the impact of biochar ageing on GHG emissions.

Biochar application can increase yield and efficiency, with a positive correlation between crop productivity and biochar application rate (Rong et al., 2023; Li et al., 2015b). This effect may be attributed to biochar's ability to improve soil physicochemical properties, thereby promoting crop growth and yield (Zhang et al., 2010). In the present study, rice yield significantly increased after biochar application and showed an upward trend with an increase in the amount of biochar applied; however, the optimum biochar application amount was not determined. With an increase in the number of application years, the yield-increasing effect of biochar decreased slightly, which differed slightly from the effect of biochar on rice-wheat rotation. In a previous study, the yield of biochar application in the first year was slightly lower than that in the third year (Wu et al., 2018). Current research on the trend of biochar yield increase lacks data support, and the results of the present study provide a reference regarding the effect of biochar application on rice yield.

4.3. Effects of biochar application duration on CH_4 metabolism in paddy fields

The results of this study showed that the last step of CH_4 production is regulated by the *mcrA* gene of methanogens, and that the *pmoA* gene is the first key enzyme encoded by methanotrophs to utilise CH_4. These two genes are commonly selected for qPCR fluorescence quantitative analysis. Previous studies have shown that the *pmoA/mcrA* ratio can be increased after biochar application (Xu et al., 2016), which is contrary to the conclusion of the present study. Studies have shown that after biochar application, the copy numbers of *pmoA* and *mcrA* genes at the rice booting stage were lower under high-biochar application rates compared to low-biochar application rates (Peng et al., 2022), which is consistent with the conclusion regarding biochar application in the first year in the present study. However, in the present study, the quantitative patterns of *pmoA* and *mcrA* genes in the eighth year of biochar application were inconsistent. This suggests that the influence of biochar on these genes may diminish over time with prolonged application.

Previous studies have shown that biochar can enhance the activity and biomass of soil microorganisms (Gao et al., 2022; Peng et al., 2022; Qin et al., 2016; Singla et al., 2014). In the present study, the community composition of methanogens and methanotrophs was similar under the same biochar application duration (Fig. 3). The results showed that, among environmental factors, a low pH was not conducive to the growth of microorganisms, and SOM and TN in soil provided nutrients for microorganisms to metabolise (Lv et al., 2022; Wang et al., 2018). In this experiment, there were significant differences in pH, SOM, and TN contents among different treatments, which may be the main factors causing the variable community structures of

Journal Pre-proof

methanogens and methanotrophs. In this study, species analysis based on the KEGG database identified *Chloroflexota* as the most abundant bacterial group. These findings differ from previously reported research conclusions. Previous research has shown that the dominant methanogens in paddy fields are archaea (*Methanosarcina*, *Horonobensis*, *Methanocellaceae*, and *Methanothrix*) (Zhang et al., 2024; Jiang et al., 2022; Wu et al., 2022; Zhou et al., 2020). However, microorganisms involved in CH_4 metabolism in soil are not restricted to the archaeal domain. At present, few studies have analysed the functional dynamics of methanogens and methanotrophs following biochar application in paddy fields. In the present study, all microorganisms involved in CH_4 metabolism and oxidation were analysed, revealing that the dominant taxa were primarily bacterial rather than archaeal. A comparative analysis of CH_4 metabolism across treatments showed that functional similarity was closely associated with biochar application duration, with treatments applied in the same year exhibiting greater functional resemblance. The CH_4 metabolic function of methanogens was less different; however, there were significant differences in the CH_4 metabolism function of methanotrophs. There was no significant difference in CH_4 metabolicsm function among treatments receiving biochar in the same year. However, CH_4 metabolic function in the first year was stronger than in the eighth year, indicating a gradual decline in CH_4 metabolism with prolonged biochar application.

5. Conclusion

The results of this experiment showed that the application of biochar improved the soil properties of paddy fields after 8 years. CH_4 emissions increased in the first year of biochar application and decreased in the eighth year of application, with lower emissions observed at higher biochar application rates across both time points. The species composition of methanogenic and methane-oxidising bacteria communities in paddy soil changed in the first year of biochar application. However, by the eighth year, the species composition of both communities showed a tendency to revert towards CK conditions. Biochar application enhanced the methane metabolism of methanogenic and methane-oxidising bacteria in rice paddies in both year 1 and year 8 and weakened over time. Additionally, biochar application increased rice yield in both year 1 and year 8. These results indicate that biochar application can improve soil fertility, reduce CH_4 emissions, change the community structure of methanogenic and methane-oxidising bacteria, and increase rice yield in the long term. While the effectiveness of biochar gradually declines over time, the impact remains significant for at least 8 years after application.

CRediT authorship contribution statement

Kai Zhang: Writing – Original Draft, Writing – Review & Editing, Conceptualization, Methodology, Investigation, Data Curation, Formal analysis. **Zhongcheng Zhang:** Writing – Original Draft, Writing – Review & Editing, Visualization, Investigation. **Yanghui Sui:** Writing –

Journal Pre-proof

Review & Editing, Supervision, Formal analysis. **Jialing Wang:** Investigation, Data Curation. **Xiaobo Pei:** Investigation, Data Curation. **Yanze Zhao:** Writing – Review & Editing. **Jiping Gao:** Writing – Review & Editing, Methodology, Conceptualization, Project administration, Funding acquisition. **Wenzhong Zhang:** Writing – Review & Editing, Supervision.

Declaration of competing interest

The authors declare that they have no known competing financial interests or personal relationships that could have appeared to influence the work reported in this paper.

Acknowledgements

This study was supported by the National Key R&D Program of China (2023YFD2301603), the Chinese Natural Sciences Foundation (31501250), and Liaoning Revitalization Talents Program (No. XLYC2007169; No. XLYC2002073).

Data Availability

Data will be made available on request.

Journal Pre-proof

References

Ali, I., Zhao, Q., Wu, K., Ullah, S., Iqbal, A., He, L., Zhang, J., Muhammad, I., Amanullah, Khan, A., Khan, A.A., Jiang, L.G., 2021. Biochar in combination with nitrogen fertilizer is a technique: to enhance physiological and morphological traits of rice (Oryza sativa L.) by improving soil physio-biochemical properties. J. Plant Growth Regul. 41 (6), 1–15. https://doi.org/10.1007/S00344-021-10454-8.

Apostolović, T., Gross, A., Rodríguez, Á.F.G., de la Rosa, J.M., Glaser, B., Knicker, H., Maletić, S., 2024. Impact of Biochar Aging on Soil Physicochemical Properties. Agronomy. 14 (12), 3007. https://doi.org/10.3390/agronomy14123007.

Bo, X.M., Zhang, Z.W., Wang, J.Y., Guo, S.M., Li, Z.T., Lin, H.Y., Huang, Y.W., Han, Z.Q., Kuzyakov, Y., Zou, J.W., 2023. Benefits and limitations of biochar for climate-smart agriculture: a review and case study from China. Biochar 5 (1), 77. https://doi.org/10.1007/s42773-023-00279-x.

Buchfink, B., Xie, C., Huson, D.H., 2015. Fast and sensitive protein alignment using DIAMOND. Nat. Methods 12 (1), 59–60. https://doi.org/10.1038/nmeth.3176.

Cao, Q.Y., Zhan, Y.W., Ding, E.Q., Gao, C.X., Zhang, L.D., Fan, X.L., 2022. Influences of alkaline fertilizer application on soil pH and soil available cadmium. J. Agro-Environ. Sci. 41 (7), 1483–1489. https://doi.org/10.11654/jaes.2021-0252.

Chen, J., Zhao, L.F., Dai, R.X., Zhang, T.J., Tang, J.J., Hu, L.L., Chen, X., 2023. Soil microbial communities of methanogens and methanotrophs in the rice-fish coculture ecosystem. Chin. J. Ecol. 42 (12), 2961–2971. https://doi.org/10.13292/j.1000-4890.202312.001.

Chen, S.F., Zhou, Y.Q., Chen, Y.R., Gu, J., 2018. fastp: an ultra-fast all-in-one FASTQ preprocessor. Bioinformatics 34 (17), i884–i890. https://doi.org/10.1093/bioinformatics/bty560.

Dai, W.N., Bao, Z.R., Meng, J., Chen, T.T., Zhang, W.T., Chen, Y.X., Li, L., Xu, S., Xue, J., 2024. Biochar incorporation increases grain yield, net ecosystem CO_2 exchange, and decreases CH_4 emissions in an alternate wetting and drying paddy ecosystem. Environ. Technol. Innov. 34, 103577. https://doi.org/10.1016/j.eti.2024.103577.

Feng, Y.F., Li, D.T., Sun, H.J., Xue, L.H., Zhou, B.B., Yang, L.Z., Liu, J.Y., Xing, B.S., 2020. Wood vinegar and biochar co-application mitigates nitrous oxide and methane emissions from rice paddy soil: a two-year experiment. Environ. Pollut. 267, 115403. https://doi.org/10.1016/j.envpol.2020.115403.

Feng, Y.Y., Feng, Y.F., Liu, Q., Chen, S., Hou, P.F., Poinern, G., Jiang, Z.T., Fawcett, D., Xue, L.H., Lam, S.S., Xia, C.L., 2022. How does biochar aging affect NH_3 volatilization and GHGs emissions from agricultural soils?. Environ. Pollut. 294, 118598. https://doi.org/10.1016/j.envpol.2021.118598.

Feng, Y.Z., Xu, Y.P., Yu, Y.C., Xie, Z.B., Lin, X.G., 2011. Mechanisms of biochar decreasing methane emission from Chinese paddy soils. Soil Biol. Biochem. 46, 80–88. https://doi.org/10.1016/j.soilbio.2011.11.016.

Fu, L.M., Niu, B.F., Zhu, Z.W., Wu, S.T., Li, W.Z., 2012. CD-HIT: accelerated for clustering the next-generation sequencing data. Bioinformatics 28 (23), 3150–3152. https://doi.org/10.1093/bioinformatics/bts565.

Gao, J.k., Liu, L., Shi, Z.Y., Lv, J.L., 2022. Biochar amendments facilitate methane production by regulating the

Journal Pre-proof

abundances of methanogens and methanotrophs in flooded paddy soil. Front. Soil Sci. 2, 801227. https://doi.org/10.3389/fsoil.2022.801227.

Gao, S.J., Liu, X.R., Li, Y.C., Liu, X.W., 2024. Effects of biochar and straw return on greenhouse gas emissions and global warming potential in the farmland. Sci. Agric. Sin. 57 (5), 935–949. https://doi.org/10.3864/j.issn.0578-1752.2024.05.009.

Heděnec, P., Alias, A., Almahasheer, H., Liu, C., Chee, P.S., Yao, M.J., Li, X.Z., Vesterdal, L., Frouz, J., Kou, Y.P., Yue, K., 2024. Global assessment of soil methanotroph abundances across biomes and climatic zones: the role of climate and soil properties. Appl. Soil Ecol. 195, 105243. https://doi.org/10.1016/j.apsoil.2023.105243.

Hyatt, D., Chen, G.L., LoCascio, P., Land, M., Larimer, F., Hauser, L., 2010. Prodigal: prokaryotic gene recognition and translation initiation site identification. BMC Bioinformatics 11 (1), 119. https://doi.org/10.1186/1471-2105-11-119.

Jiang, M.D., Xu, P., Wu, L., Zhao, J.S., Wu, H.T., Lin, S., Yang, T.W., Tu, J.M., Hu, R.G., 2022. Methane emission, methanogenic and methanotrophic communities during rice-growing seasons differ in diversified rice rotation systems. Sci. Total Environ. 842, 156781. http://doi.org/10.1016/j.scitotenv.2022.156781.

Jin, P.H., Chen, Z., Wang, H., Lv, R.J., Hu, T.L., Zhou, R., Zhang, J.R., Lin, X.W., Liu, Q., Xie, Z.B., 2024. 12-year continuous biochar application: mitigating reactive nitrogen loss in paddy fields but without rice yield enhancement. Agric. Ecosyst. Environ. 375, 109223. https://doi.org/10.1016/j.agee.2024.109223.

Khan, Z., Zhang, K.K., Khan, M.N., Zhu, K.M., Hu, L.Y., 2024. Effects of biochar persistence on soil physiochemical properties, enzymatic activities, nutrient utilization, and crop yield in a three-year rice-rapeseed crop rotation. Eur. J. Agron. 154, 127096. https://doi.org/10.1016/j.eja.2024.127096.

Khan, Z., Zhang, K.K., Khan, M.N., Zhu, K.M., Hu, L.Y., 2024. Effects of biochar persistence on soil physiochemical properties, enzymatic activities, nutrient utilization, and crop yield in a three-year rice-rapeseed crop rotation. Eur. J. Agron. 154, 127096. https://doi.org/10.1016/j.eja.2024.127096.

Li, D.D., He, H., Pan, F.F., Yang, S.Y., 2023. Effects of biochar application on greenhouse gas emissions and yield in a double-season rice cropping system under various optimized nitrogen reduction conditions. J. Agro-Environ 42 (11), 2625–2634. https://doi.org/10.11654/jaes.2023-0050.

Li, D.H., Liu, C.M., Luo, R.B., Sadakane, K., Lam, T.W., 2015. MEGAHIT: an ultra-fast single-node solution for large and complex metagenomics assembly via succinct de bruijn graph. Bioinformatics 31 (10), 1674–1676. https://doi.org/10.1093/bioinformatics/btv033.

Li, L., Zhou, Z, Q., Pan, X.J., Li, B., Xiong, Z.Q., 2015a. Combined effects of nitrogen fertilization and biochar incorporation on methane and nitrous oxide emissions from paddy fields in rice-wheat annual rotation system. J. Plant Nutr. Fert. 21 (5), 1095–1103. https://doi.org/10.11674/zwyf.2015.0501.

Li, L., Zhou, Z.Q., Pan, X.J., Xiong, Z.Q., 2015b. Effects of biochar on N_2O and CH_4 emissions from paddy field under rice-wheat rotation during rice and wheat growing seasons relative to timing of amendment. Acta Pedol. Sin. 52 (4), 839–848. https://doi.org/10.11766/trxb201407160357.

Li, R.Q., Li, Y.R., Kristiansen, K., Wang, J., 2008. SOAP: short oligonucleotide alignment program. Bioinformatics 24 (5), 713–714. https://doi.org/10.1093/bioinformatics/btn025.

Journal Pre-proof

Li, X., Wu, D., Liu, X., Huang, Y.p., Cai, A.D., Hu, X., Ran, J.W., Xiao, J., Zhang, W.J., 2024. A global dataset of biochar application effects on crop yield, soil properties, and greenhouse gas emissions. Sci. Data 11 (1), 57. https://doi.org/10.1038/S41597-023-02867-9.

Liu, H., Jiao, Y., Dou, W.Y., Zhang. W.L., Pei, W., 2024. Compensation effect and mechanism of nitrogen reduction combined with biochar application on soil fertility and rice yield. Trans. Chin. Soc. Agric. Mach. 55 (9), 391–401+469. https://doi.org/10.6041/j.issn.1000-1298.2024.09.034.

Liu, Q., Li, Y.H., Liu, S.L., Gao, W., Shen, J.L., Zhang, G.B., Xu, H., Zhu, Z.K., Ge, T.D., Wu, J.S., 2021. Anaerobic primed CO_2 and CH_4 in paddy soil are driven by Fe reduction and stimulated by biochar. Sci. Total Environ. 808, 151911. https://doi.org/10.1016/j.scitotenv.2021.151911.

Long, X.X., Yu, Z.N., Liu, S.W., Gao, T., Qiu, R.L., 2024. A systematic review of biochar aging and the potential eco-environmental risk in heavy metal contaminated soil. J. Hazard. Mater. 472, 134345. https://doi.org/10.1016/j.jhazmat.2024.134345.

Luo, D., Li, Y.Y., Yao, H.Y., Chapman, S.J., 2022. Effects of different carbon sources on methane production and the methanogenic communities in iron rich flooded paddy soil. Sci. Total Environ. 823, 153636. http://dx.doi.org/10.1016/j.scitotenv.2022.153636.

Luo, S.S., Wang, S.J., Tian, L., Li, S.Q., Li, X.J., Shen, Y.F., Tian, C.J., 2017. Long-term biochar application influences soil microbial community and its potential roles in semiarid farmland. Appl. Soil Ecol. 117–118, 10–15. https://doi.org/10.1016/j.apsoil.2017.04.024.

Lv, Y.D., Xu, L.Q., Guo, X.H., Liu, J.J., Zou, B., Guo, Y.K., Zhang, Y.F., Li, H.Y., Zheng, G.P., Guo, Y.X., Zhao, M.H., 2022. Effect of biochar on soil physiochemical properties and bacterial diversity in dry direct-seeded rice paddy fields. Agronomy 13 (1), 4. https://doi.org/10.3390/agronomy13010004.

Nan, Q., Hu, S.L., Qin, Y., Wu, W.X., 2021. Methane oxidation activity inhibition via high amount aged biochar application in paddy soil. Sci. Total Environ. 796, 149050. https://doi.org/10.1016/j.scitotenv.2021.149050.

Noguchi, H., Park, J., Takagi, T., 2006. MetaGene: prokaryotic gene finding from environmental genome shotgun sequences. Nucleic Acids Res. 34 (19), 5623–5630. https://doi.org/10.1093/nar/gkl723.

Patel, S.K.S., Shanmugam, R., Kalia, V.C., Lee, J.K., 2020. Methanol production by polymer-encapsulated methanotrophs from simulated biogas in the presence of methane vector. Bioresour. Technol. 304, 123022. https://doi.org/10.1016/j.biortech.2020.123022.

Peng, D.Y., Yang, S.H., Li, W.Z., LI, M., Dai, H.D., Zhou, J.Y., 2022. Effects of biochar application on methane-producing and oxidizing bacteria in water-saving irrigation paddy fields. Water Saving Irrig. (5), 54–59. https://doi.org/10.3969/j.issn.1007-4929.2022.05.009.

Perry, H., Carrijo, D.R., Duncan, A.H., Fendorf, S., Linquist, B.A., 2024. Mid-season drain severity impacts on rice yields, greenhouse gas emissions and heavy metal uptake in grain: evidence from on-farm studies. Field Crop. Res. 307, 109248. https://doi.org/10.1016/j.fcr.2024.109248.

Qi, J.Q., Yuan, H.Y., Zhuang, Q.L., Zama, E.F., Tian, X.F., Tao, B.X., Zhang, B.H., 2023. Effect of different types of biochar on soil properties and functional microbial communities in rhizosphere and bulk soils and their relationship with CH_4 and N_2O emissions. Front. Microbiol. 14, 1292959.

Journal Pre-proof

https://doi.org/10.3389/fmicb.2023.1292959.

Qi, L., Ma, Z.L., Chang, S.X., Zhou, P., Huang, R., Wang, Y.Y., Wang, Z.F., Gao, M., 2021. Biochar decreases methanogenic archaea abundance and methane emissions in a flooded paddy soil. Sci. Total Environ. 752, 141958. https://doi.org/10.1016/j.scitotenv.2020.141958.

Qin, X.B., Li, Y., Wang, H., Liu, C., Li, J.L., Wan, Y.F., Gao, Q.Z., Fan, F.L., Liao, Y.L., 2016. Long-term effect of biochar application on yield-scaled greenhouse gas emissions in a rice paddy cropping system: a four-year case study in south China. Sci. Total Environ. 569–570, 1390–1401. https://doi.org/10.1016/j.scitotenv.2016.06.222.

Quilliam, S.R., Glanville, C.H., Wade, C.S., Jones, D.L., 2013. Life in the 'charosphere' – does biochar in agricultural soil provide a significant habitat for microorganisms?. Soil Biol. Biochem. 65, 287–293. https://doi.org/10.1016/j.soilbio.2013.06.004.

Rong, F.L., Qin, S.S., Su, G.R., Wu, L.Q., Wu, A.Q., Wang, X.H., Zhang, M.Y., Chen, F.L., 2023. Legacy effect of single biochar application on soil ecosystem multifunctionality and its contribution to rice yield: a five-year field experiment for acidic paddy. Field Crop. Res. 303, 109141. https://doi.org/10.1016/j.fcr.2023.109141.

Schorn, S., Graf, J.S., Littmann, S., Hach, P.F., Lavik, G., Speth, D.R., Schubert, C.J., Kuypers, M.M.M., Milucka, J., 2024. Persistent activity of aerobic methane-oxidizing bacteria in anoxic lake waters due to metabolic versatility. Nat. Commun. 15 (1), 5293. https://doi.org/10.1038/s41467-024-49602-5.

Shahid, I., Xu J.C., Sehroon, K., Ruth, W.F., Zaman, K.H., Sadia, N., Sailesh, R., 2023. Regenerative fertilization strategies for climate-smart agriculture: consequences for greenhouse gas emissions from global drylands. J. Clean Prod. 398. https://doi.org/10.1016/j.jclepro.2023.136650.

Shrestha, R.K., Jacinthe, P.A., Lal, R., Lorenz, K., Singh, M.P., Demyan, S.M., Ren W., Lindsey L.E., 2023. Biochar as a negative emission technology: a synthesis of field research on greenhouse gas emissions. J. Environ. Qual. 52 (4), 769–798. https://doi.org/10.1002/jeq2.20475.

Singla, A., Dubey, S.K., Singh, A., Inubushi, K., 2014. Effect of biogas digested slurry-based biochar on methane flux and methanogenic archaeal diversity in paddy soil. Agric. Ecosyst. Environ. 197, 278–287. https://doi.org/10.1016/j.agee.2014.08.010.

Spokas, K.A., 2013. Impact of biochar field aging on laboratory greenhouse gas production potentials. GCB Bioenergy 5 (2), 165–176. https://doi.org/10.1111/gcbb.12005.

Tian, Q., Liu, Y.J., Hu, R.W., Yang, K., Zheng, B.F., Li, J.h., Liu, Z.X., Li, P., Ma, T.T., Xiong, K.L., Liang, J.S., Rang, Z.W., Li, J., 2024. Reduction of soil methane emissions from croplands with 20–40 years of cultivation mediated by methane-metabolizing microorganisms. J. Clean Prod.435, 140489. https://doi.org/10.1016/j.jclepro.2023.140489.

Wang, C., Chen, D., Shen, J.L., Yuan, Q., Fan, F.L., Wei, W.X., Li, Y., Wu, J.S., 2021. Biochar alters soil microbial communities and potential functions 3–4 years after amendment in a double rice cropping system. Agric. Ecosyst. Environ. 311, 107291. https://doi.org/10.1016/j.agee.2020.107291.

Wang, M.J., Jiang, W.T., Xu, Y.X., Liu, Y.X., Lv, H.H., Wang, Y.Y., Yang, S.M., He, L.L., Cai, Y.J., 2024. Effects of long-term biochar addition on denitrification N_2O emissions from bacteria fungi in paddy soil. Environ. Sci. 45 (08), 4923–4931. https://doi.org/10.13227/j.hjkx.202309176.

Journal Pre-proof

Wang, M.Y., Xu, X.P., Wang, W, Q., Wang, G.L., Su, C.J., 2018. Effects of slag and biochar amendments on methanogenic community structures in paddy fields. Acta Ecol. Sin. 38 (8), 2816–2828. https://doi.org/10.5846/stxb201705210939.

Wang, X.J., Liu, J.R., Li, R.L., Wang, S.C., Ma, J., Zhu, Z.K., Zhang, G.B., Xu, H., 2024. The impact of nitrogen application rate on rice yield and greenhouse gas emissions of ratoon rice in the taihu lake region. Chin. J. Eco-Agric 1–13. https://doi.org/10.12357/cjea.20240093.

Wang, Z.J., Wang, H.H., Li, J.Q., Wu, Y.Z., Fu, P.J., Meng, L., Tang, S.R., 2021. Effects of coconut chaff biochar amendment on methane and nitrous oxide emissions from paddy fields in hot areas. Environ. Sci. 42 (8), 3931–3942. https://doi.org/10.13227/j.hjkx.202011247.

Wu, J.F., Ma, C.L., Li, F.S., 2022. Microbial community structure and function in paddy soil as affected by water-saving irrigation mode. Eur. J. Soil Biol. 113, 103450. https://doi.org/10.1016/j.ejsobi.2022.103450.

Wu, Z., Dong, Y.B., Xiong, Z.Q., 2018. Effects of biochar application three-years ago on global warming potentials of CH_4 and N_2O in a rice-wheat rotation system. Chin. J. Appl. Ecol. 29 (1): 141–148. https://doi.org/10.13287/j.1001-9332.201801.028.

Wu, Z., Sun, L.Y., Dong, Y.B., Xu, X.T., Xiong, Z.Q., 2022. Contrasting effects of different field-aged biochars on potential methane oxidation between acidic and saline paddy soils. Sci. Total Environ. 853, 158643. https://doi.org/10.1016/j.scitotenv.2022.158643.

Xin, D.H., Li W.L., Choi, J., Yu, Y.H., Chiu, P.C., 2023. Pyrogenic black carbon suppresses microbial methane production by serving as a terminal electron acceptor. Environ. Sci. Technol. 57 (49), 20605–20614. https://doi.org/10.1021/acs.est.3c05830.

Xu, X., Chen, C., Xiong, Z.Q., 2016. Effects of biochar and nitrogen fertilizer amendment on abundance and potential activity of methanotrophs and methanogens in paddy field. Acta Pedol. Sin. 53 (6), 1517–1527. https://doi.org/10.11766/trxb201604210087.

Yu, H.Y., Zhang, X.C., Meng, X.T., Luo, D., Liu, X.H., Zhang, G.B., Zhu, C.W., Li, Y.Y., Yu, Y.X., Yao, H.Y., 2023. Methanogenic and methanotrophic consortia determine lower CH_4 fluxes in a subtropical paddy field under long-term elevated CO_2. Sci. Total Environ. 904, 166904. https://doi.org/10.1016/j.scitotenv.2023.166904.

Zhang, A., Cui, L.Q., Pan, G.X., Li, L.Q., Hussain, Q., Zhang, X.H., Zheng, J.W., Crowley, D., 2010. Effect of biochar amendment on yield and methane and nitrous oxide emissions from a rice paddy from tai lake plain, China. Agric. Ecosyst. Environ. 139 (4), 469–475. https://doi.org/10.1016/j.agee.2010.09.003.

Zhang, X.X., Lv, Z.P., Sun, H.F., Bi, J.G., Zhang, J.N., Wang, C., Zhou, S., 2024. Crosstalk between methanogens and methanotrophs determines methane emissions in a rice paddy under different watering regimes. Appl. Soil Ecol. 195, 105229. https://doi.org/10.1016/j.apsoil.2023.105229.

Zhao, Y.Z., Jiang, H.F., Gao, J.P., Feng, Y.Y., Yan, B.C., Li, K., Lan, Y., Zhang, W.Z., 2023. Effects of nitrogen co-application by different biochar materials on rice production potential and greenhouse gas emissions in paddy fields in northern China. Environ. Technol. Innov. 32, 103242. https://doi.org/10.1016/j.eti.2023.103242.

Zhao, Y.Z., Jiang, H.F., Gao, J.P., Wan, X., Yan, B.C., Liu, Y., Cheng, G.Q., Chen, L.Q., Zhang, W.Z., 2024. Effects of biochar application methods on greenhouse gas emission and nitrogen use efficiency in paddy fields. Sci.

Journal Pre-proof

Journal Pre-proof

Total Environ. 915, 169809. https://doi.org/10.1016/j.scitotenv.2023.169809.

Zhou, G.P., Gao, S.J., Xu, C.X., Zeng, N.H., Rees, R.M., Cao, W.D., 2020. Co-incorporation of Chinese milk vetch (Astragalus sinicus L.) and rice (Oryza sativa L.) straw minimizes CH_4 emissions by changing the methanogenic and methanotrophic communities in a paddy soil. Eur. J. Soil Sci. 71 (5), 924–939. https://doi.org/10.1111/ejss.12930.

Zhou, Y.C., Wu, L.L., Li, D.Y., Guo, S.B., Chen, Z.M., Li, Z.L., Zhao, Y., 2023. Review on the long-term and short-term effects of biochar addition on soil greenhouse gas emissions. Environ. Sci. 44 (8), 4742–4750. https://doi.org/10.13227/j.hjkx.202207066.

CRediT authorship contribution statement

Kai Zhang: Writing – Original Draft, Writing – Review & Editing, Conceptualization, Methodology, Investigation, Data Curation, Formal analysis. **Zhongcheng Zhang:** Writing – Original Draft, Writing – Review & Editing, Visualization, Investigation. **Yanghui Sui:** Writing – Review & Editing, Supervision, Formal analysis. **Jialing Wang:** Investigation, Data Curation. **Xiaobo Pei:** Investigation, Data Curation. **Yanze Zhao:** Writing – Review & Editing. **Jiping Gao:** Writing – Review & Editing, Methodology, Conceptualization, Project administration, Funding acquisition. **Wenzhong Zhang:** Writing – Review & Editing, Supervision.

Declaration of Interest Statement

The authors declare that they have no known competing financial interests or personal relationships that could have appeared to influence the work reported in this paper.

Journal Pre-proof

Graphical abstract

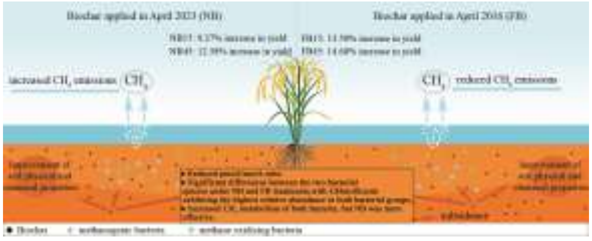

Highlights

1. Corn straw biochar application improved the physical and chemical properties of the soil in both the first year (NB) and the eighth year (FB).
2. NB15, NB45, FB15, and FB45 increased rice yield by 9.27%, 12.58%, 13.50%, and 14.68%, respectively.
3. NB increased CH_4 emissions, FB decreased CH_4 emissions, and CH_4 emissions were higher at low biochar application than at high biochar application at different application years.
4. NB and FB soils differed significantly in methanogenic and methane-oxidising bacterial species, with *Chloroflexota* exhibiting the highest relative abundance in both bacterial groups, and NB and FB reduced the *pmoA/mcrA* ratio in soils.
5. NB and FB enhance CH_4 metabolism by methanogenic and methane-oxidising bacteria in soil.

Journal Pre-proof